Quantum diffraction and threshold law for the Temkin-Poet model of electron-hydrogen ionization

Naoyuki Miyashita, Daiji Kato,* and Shinichi Watanabe
Department of Applied Physics and Chemistry, University of Electro-Communications, 1-5-1, Chofu-ga-oka, Chofu-shi, Tokyo 182-8585, Japan
(Received 8 October 1998)

Relying on an entirely *ab initio* quantum-mechanical scheme, we investigate the threshold behavior of a model electron-impact ionization problem in which the target hydrogen atom interacts with the incident electron only by monopole. The total ionization cross section for a singlet is shown to follow the threshold law of an exponential form as proposed by Macek and Ihra [Phys. Rev. A **55**, 2024 (1997)], thus supporting the argument based on the local instability of the ''ridge'' motion despite the reported absence of classical ridge trajectories. Below the classical threshold, quantum diffraction allows the two electrons to have a large probability amplitude in the region inaccessible to the classical trajectories. The energy distribution for singlet in final continuum channels is shown to have a hitherto unexpected V-shaped structure at energies between 0 and 1 a.u. above the ionization threshold. The V structure becomes sharper toward the threshold while it approaches the quadratic form surmised by Bray [Phys. Rev. Lett. **78**, 4721 (1997)] at higher energies.
[S1050-2947(99)02206-4]

PACS number(s): 34.50.Fa, 31.15.Ja

It has been a great challenge to devise and implement an *ab initio* quantum-mechanical scheme for electron-impact ionization close to the threshold. We believe that most of this goal is being achieved [1–3] and that time is ripe for exploring further details of the ionization process and exposing quantum-mechanical effects which lie beyond classical or semiclassical treatments. We present a consolidating example, and eventually point out as a subject for future studies a phenomenon that appears to fall beyond the original mode of analysis exploited by Wannier [4] and advanced by Rau [5], Peterkop [6], Fano [7], Watanabe [8], Macek and Ihra [9] and other more recent authors [10]. In so doing, we shall deal with the model hydrogen atom which interacts with the incident electron only by the monopole term. (The real hydrogen atom has been dealt with elsewhere [2,3].) This model atom, due to Temkin [11] and Poet [12], provides a step in the analysis of electron-electron correlations. The benchmark calculations in [12] may be used for accessing the accuracy of a numerical scheme. The model is undoubtedly an oversimplified system, yet it poses some key theoretical questions. One intriguing feature of the Temkin-Poet model is that the classical trajectories that would lead to ionization are absent below a finite energy ($E<E_{\rm cl}=0.166\ldots$ a.u.) [13]. Any theory based on classical trajectories thus do not apply below the delayed onset energy, that is, a truly quantum aspect of the ionization problem becomes exposed below the classical threshold. It is also worthwhile to note that no experimental investigation on this quantum feature is possible since the Temkin-Poet model represents a nonexistent system. This model problem can be investigated only by a well-founded theoretical scheme as an alternative to a laboratory experiment.

Our separate technical paper [3] presents an *ab initio* quantum-mechanical scheme. Converged ionization cross sections are obtained over a wide energy range without the burden of a large-scale diagonalization or linear algebra required of other methods. It divides the configuration space into small subregions, solves the Schrödinger equation in each subregion as accurately as possible by an ingenuous variational scheme, and then patches up the solutions to deduce the scattering matrix. The paper also highlights major achievements of the method such as the *ab initio* reproduction of the Wannier threshold exponent for fixed angular degrees of freedom, the observation of the binary encounter peak at moderate energies, and of the uniform energy distribution near the threshold, etc.

It is worthwhile to give an overview of the Wannier theory. An inspiring aspect of Wannier's analysis is to have identified the relative importance of the kinetic and Coulomb potential energy as well as the conspicuous role played by the potential ridge. He classified the configuration space into three parts: the first one is the reaction zone where the seed of ionization takes place in the proximity of the nucleus, the second is the Coulomb zone which is dominated by the potential energy, and the last is the asymptotic zone where the kinetic energy dominates. The asymptotic zone thus lies beyond $R=\sqrt{r_1^2+r_2^2}=1/E$. In the Wannier theory, the threshold exponent derives from the rate of flux loss from the potential ridge in the Coulomb zone, but it is believed to be unaffected by the dynamics in the asymptotic zone. Paradoxically, Wannier's solutions being restricted to the Coulomb zone, it cannot deduce what happens in the asymptotic zone. It is thus worthwhile to examine the behavior of the two continuum electrons beyond the Coulomb zone and thus to appreciate the limitation of Wannier's treatment.

It is clear from the following argument that the behavior of the wave function should differ between the Coulomb and asymptotic zones. At low energies, the two electrons must maintain near the ridge a dynamically unstable configuration

*Present address: Japan Science and Technology Corporation, International Project ''Cold Trapped Ions,'' Axis-Choufu Bldg. 3F, 1-40-2 Fuda, Choufu-shi, Tokyo 182-0024, Japan.

TABLE I. Comparison of various estimates of the parameters γ and σ_0 in $\sigma=\sigma_0\exp(-\gamma E^{-1/6})$. The numerically determined values using two different fitting procedures are consistent with the semiquantal estimates. Fitting 1 is by the singular-value decomposition method and Fitting 2 is by a nonlinear fitting procedure. See text for the specific functional form. Numbers in parentheses represent approximately the uncertainties in the obtained values.

	Analytical	WKB	Other theory [9]	Fitting 1	Fitting 2
γ	6.30	6.89	6.87	6.65 (0.03)	6.75 (0.02)
σ_0				80 (1)	104 (1)

$\vec{p}_1=-\vec{p}_2$ where $\vec{p}_1$ and $\vec{p}_2$ are their momenta. Once in the asymptotic zone, the two electrons can proceed to infinity as a pair of free particles, thus maintaining merely the ratio p_1/p_2. Consequently, the wave function attains a constant profile with respect to $\alpha_p=\tan^{-1}(p_1/p_2)$ in the momentum space pseudoangle or to $\alpha=\tan^{-1}(r_1/r_2)$ in the configuration space. This dependence on the hyperspherical pseudoangle is different from the dependence on the scaled pseudoangle in the Coulomb zone. For instance, the solution depends on $\beta=R^{1/4}(\pi/4-\alpha)$ in the case of the ionization of the real hydrogen atom, and on $\beta=R^{1/3}(\pi/4-\alpha)$ in the case of the Poet-Temkin model. In short, this explicit dependence on R is not obeyed asymptotically.

The cusp of the Temkin-Poet model potential at the ridge leads to the exponential threshold law [9] reflecting its steepness. Let us outline this result step by step. The outgoing-wave boundary condition on the channel function along α represents the instability of the ridge motion, leading to an optical potential of the form $(a+ib)/R^{4/3}$ [14], where a and b are both real [15]. The imaginary part of the WKB-type phase integral

$$\mathrm{Im}\int^{\tilde{R}}\sqrt{\frac{2C_0}{R}+\frac{2(a+ib)}{R^{4/3}}}dR\simeq\frac{\gamma}{2}\tilde{R}^{1/6}, \tag{1}$$

where $\gamma=12b/\sqrt{2C_0}>0$, represents the decline in amplitude of the ionizing component astride the ridge, hence the ionization cross section is expected to scale as $\exp(-\gamma E^{-1/6})$. (Here in the WKB-type integral we have dropped E from the real part because $C_0/R\gg E$ in the Coulomb zone.) One may evaluate the coefficients a and b analytically using the Airy functions or approximately by the WKB representation [14]. The value of the parameter γ so evaluated is tabulated in Table I.

Let us present an *ab initio* quantum result that strongly supports the exponential threshold law for singlet, forgoing far more strenuous calculations required of triplet. Figure 1 shows the ionization cross sections for singlet in the energy region between 0 and 2 a.u. excess energy, the lower limit for our numerical implementation being 0.001 a.u. The cross sections converged at worst to three digits for the matching radius $R_m=4000$–5000 a.u., which is about 4 to 5 times greater than $1/E_{\min}$. The near-threshold region is presented as a log-log plot in the inset. It is known that another quantum conjecture due to Temkin [16] is a power law $\sigma\propto E^{1.5}$. Recent *ab initio* quantum calculations elucidated that *ab initio* results do not fit Temkin's. Instead, they unexpectedly fit to E^2 as well as to the exponential law; Robicheaux *et al.* [17] and Scott *et al.* [18] attempted to confirm the exponential threshold law, but did not reach an unequivocal conclusion largely due to a considerable amount of fluctuating uncertainty in the cross sections at low energies. In the present results, there is no denying that the cross section vanishes toward the threshold at a rate faster than any given power law because the plot has a nonvanishing curvature at any energy without a hint of achieving a constant slope. The numerical cross sections are fitted to the analytical expression

$$\sigma=\exp[-\gamma E^{-\lambda}+G(E)], \tag{2}$$

where $G(E)=\Sigma_{n=0}^{N}a_nE^n$ is to represent nonsingular energy corrections away from $E=0$. Macek and Ihra [9] argued that the exponent λ be 1/6. This value being crucial to the proceeding fitting, we determine it by first neglecting the slow variation of $G(E)$, thus

$$\lambda\simeq-\frac{y''}{y'}E-1, \tag{3}$$

where, $y=\ln\sigma$, $y'=dy/dE$, and $y''=d^2y/dE^2$. As shown in Fig. 2, there is a marginal scatter in the numerically evaluated λ. By performing the least-squares fitting we get $\lambda=0.149(\pm0.008)+2.34(\pm0.223)E$. Extrapolating to $E=0$ then leads to

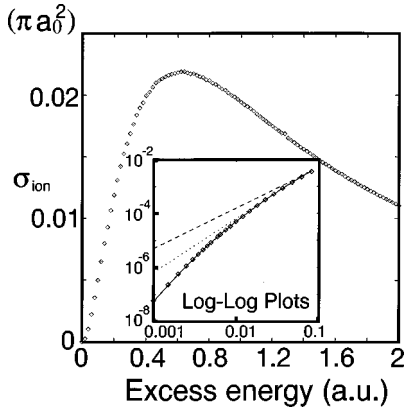

FIG. 1. The total ionization cross section of singlet over an extended energy range near and below the classical threshold ($E<E_{\mathrm{cl}}=0.166\ldots$ a.u.). The inset is a log-log plot magnifying the region of the exponential behavior. The diamonds represent the numerically obtained cross sections, the *solid* curve represents the exponential law, $\sigma_0\exp(-\gamma E^{-1/6})$ with $\gamma=6.75$ and $\sigma_0=104$ which are obtained by a nonlinear fitting to the numerically obtained cross sections (see text and Table I), the *broken* line Temkin's power law, $\propto E^{1.5}$, and the *dotted* line $\propto E^2$ [17,18].

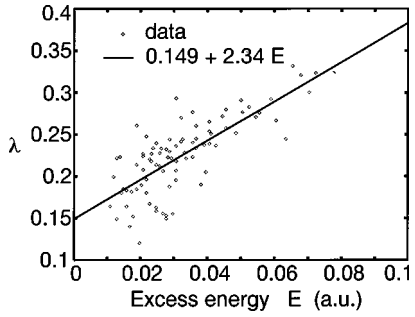

FIG. 2. The relation between excess energy and λ. By setting $y=\ln\sigma$, we get $\lambda=-(y''/y')E-1$. The *solid* line shows the energy dependence of λ determined by least-squares fitting, $\lambda=0.149(\pm0.008)+2.34(\pm0.223)E$. The value of λ approaches $0.149(\pm0.008)$ as $E\to0$ which is 10% smaller than the WKB estimate.

$$\lambda\sim0.149(\pm0.008), \tag{4}$$

which is about 10% smaller than $\lambda=1/6\simeq0.167$. From here on, we presume the value of λ to be either 1/6 or 0.149 as obtained by fitting. We extract γ in two ways. One is a fitting to the form

$$E^{\lambda+1}\ln\sigma=-\gamma E+E^{\lambda+1}G(E), \tag{5}$$

where the powers of E included in $G(E)$, namely N, is chosen large enough for γ and a_0 to converge within four significant digits. The solution set is stably obtained by means of the singular-value decomposition method. The other is a nonlinear fitting to σ of Eq. (2) with $N=3$. In both procedures, the fitted value of γ becomes stabilized as the minimum energy $E_{\min}$ is lowered. We carried out our calculations down to $E_{\min}=0.001$ a.u. in order to attain a convincing convergence of γ within two significant digits. In Table I, we show our least-squares fitting to the numerically evaluated total ionization cross section for singlet. For the present value of $\lambda=1/6$, this table reveals the numerically fitted value of γ to be in good agreement with the one deduced by the Wannier-type arguments. For $\lambda=0.149$, an independent fitting yields $\gamma=8.4(\pm0.1)$ which is about 20% larger in magnitude than that for $\lambda=1/6$. The quantities λ and γ are thus found to strongly support the exponential threshold law, Eq. (5).

Now that we have demonstrated the validity of the exponential law, we consider situations where semiclassical methods based entirely on classical trajectories [19] are inapplicable. Since there is no trace of delayed threshold [13] in the quantum results, one may attribute the disappearance of the sharp classical threshold to quantum diffraction which tend to blur sharp edges in the classical phase space. This point is in contrast with the conclusion of Rost [19] that the two-electron escape near the threshold is a classical process in the case of the collinear hydrogen atom. A strong support of the quantum diffraction lies in the global comportment of the wave function. For this purpose, we generated a set of plots using a simple approximate procedure introduced by Poet [12]. The solution is constructed by superposing solutions that solve the Schrödinger equation in each of the half spaces, $r_1<r_2$ and $r_1>r_2$. The condition for a global solution is that it satisfies the symmetric or antisymmetric boundary condition with respect to $r_1=r_2$. The production of the wave function is done only for singlet on account of its predominance near threshold. To stabilize the solution, we modified the Poet method slightly; we restricted the solution space to a finite box, and then extracted the ionization component. The accuracy is monitored by the unitarity of the S matrix and by comparing the energy distribution against our more rigorous procedure. Figures 3(a)–3(f) represent the ionization components of the wave function generated at representative energies, $E=0.25$ a.u. which is above $E_{\rm cl}$, $E=0.167$ a.u. which is close to $E_{\rm cl}$, and $E=0.05$ a.u. which is below $E_{\rm cl}$, respectively, and are pairwise plotted with respect to two alternative sets of radial variables. Note in passing that the excitation components are unequivocally removed by projecting onto the excited target states in the asymptotic region, $R\gg1/E$. The pair of solid curves indicate the classical trajectories that originate from $r_1=r_2=1/E$ and become parallel to either the r_1 or r_2 axis in the asymptotic limit, thus they represent zero-energy escape passing through the critical location in the configuration space, $r_1=r_2=1/E$, and mark the boundary of the ionizing trajectories [13]. The top row, (a)–(c), represents the wave functions with respect to r_1 and r_2, meanwhile the lower one, (d)–(f), are with respect to Er_1 and Er_2 so that the point $r_1=r_2=1/E$ remains fixed in each panel. What the top panels show is that the region of quantum diffraction in the Coulomb zone, $r_1,r_2<1/E$, grows as the total energy lowers toward the ionization threshold $E=0$. On the other hand, with respect to the scaled radial variables which maintain the relevant dynamical scale invariant, the wave function appears to concentrate toward the ridge as the energy lowers. We also observe that throughout these panels, the classical trajectories as defined in Ref. [13] mark the asymptotic region quite well.

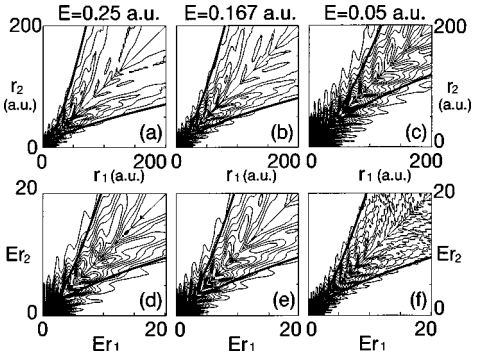

FIG. 3. Ionization component of the wave function for singlet at representative energies. (a) and (d) are at $E=0.25$ a.u. above the classical ionization threshold $E_{\rm cl}$, (b) and (e) at $E=0.167$ a.u. near $E_{\rm cl}$, and (c) and (f) at $E=0.05$ a.u. below $E_{\rm cl}$. (a)–(c) are plotted with respect to r_1 and r_2; (d)–(f) with respect to Er_1 and Er_2. The pair of *solid* curves mark the ionizing classical trajectories corresponding to zero-energy escape originating from $r_1=r_2=1/E$. Note the larger quantum diffraction in the Coulomb zone as the energy lowers.

In Fig. 4, we show the energy distribution of singlet (a) and triplet (b) at $E=1.0$ a.u. obtained by two separate procedures. One is from the numerical wave function Ψ evaluated at the asymptotic matching hyperradius R_m. Within the validity of the stationary-phase approximation (SPA) a constraint $\alpha=\alpha_p$ obtains, thus a relation between the asymptotic

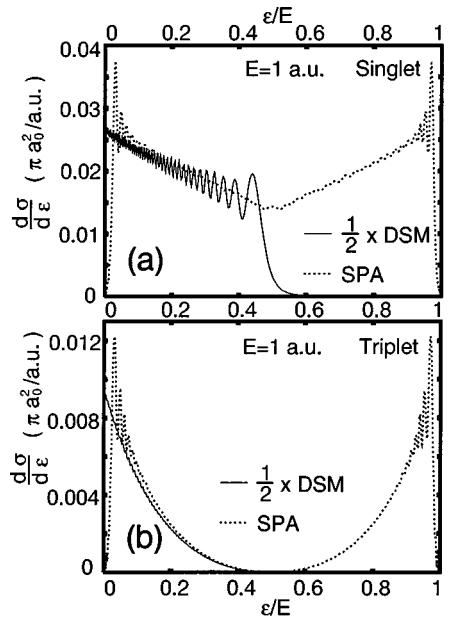

FIG. 4. Energy distribution between the electron pair at $E=1$ a.u., (a) for the singlet and (b) for the triplet. The *dotted* line represents the SPA distribution calculated using Eq. (6) with the numerically obtained asymptotic wave function, and the *solid* line shows the DSM result divided by 2 for comparison. This result is in good agreement with Ref. [1].

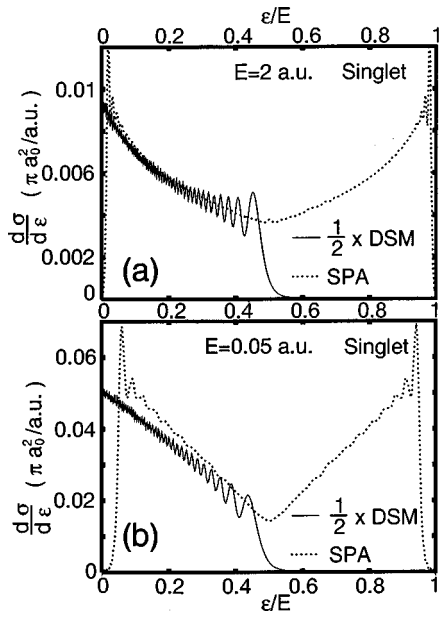

FIG. 5. Same as Fig. 4, (a) for $E=2$ a.u. above $E_{\rm cl}$ and (b) for $E=0.05$ a.u. below $E_{\rm cl}$. Note how the approximately quadratic dependence is taken over by the markedly linear V-shaped dependence.

wave function Ψ and the S matrix reduces to, according to [20]

$$|S|^2=\frac{\pi(4\pi)^2}{K}\frac{|\Psi|^2}{\sin 2\alpha_p}, \tag{6}$$

where S represents the S matrix, $K=\sqrt{2E}$ and the other variables have already been defined. The other procedure is to use the S matrix directly obtained by the two-dimensional matching of the numerical wave function to the approximate asymptotic solutions of direct product form [3]. Let us refer to the latter direct cross section as the direct S-matrix method (DSM). The point of producing the two sets of results here is not only to ascertain the consistency of the results but to take advantage of the stationary-phase approximation (SPA) which appears to yield an energy distribution closer in shape to the correct asymptotic limit (note its generally fewer oscillatory structures and its automatically satisfied symmetry with respect to $\epsilon_1=\epsilon_2$). Incidentally, the oscillations in the energy distribution are nothing but an artifact of the finite matching radius. Figure 4 indicates a good agreement between SPA and DSM. Energy distribution at this energy was previously calculated by Bray [1] and is in good agreement with ours.

In Fig. 5, we show energy distribution for singlet at $E=2.0$ a.u. ($>E_{\rm cl}$) and $E=0.05$ a.u. ($<E_{\rm cl}$) obtained by both SPA and DSM. One remarkable feature of the distribution at moderate to low energies (below about 1 a.u. but not necessarily below the classical threshold) is its V shape as in Fig. 5(b). Only in the neighborhood of $\epsilon_1=\epsilon_2$, does it flatten due to the symmetry requirement. This feature becomes sharper toward the threshold. At moderately high energies, however, the distribution has a shape which is somewhat suggestive of the V shape but its overall features may be described as quadratic [1] as in Fig. 5(a). That the peak should occur away from $\epsilon_1=\epsilon_2$ is readily accountable. First, the ionization amplitude astride the ridge decays exponentially beyond $R=1/E$. Second, the ionizing trajectories leaving the ridge make some finite angle with it. These two points suggest a concentration of the distribution toward greater differences in energy. What would be nontrivial is to unravel the physical origin of the high degree of linearity because the local solution in the Coulomb zone does not lead readily to this behavior. No analytical solution is currently available for this problem. It must be recalled that even for the better known ''true'' hydrogen the correct energy distribution is reproduced only numerically [21].

To summarize, the nontrivial connection between the dynamics prevalent in the Coulomb zone and that in the asymptotic zone is made particularly articulate for the present Temkin-Poet potential that has a cusp at $r_1=r_2$. A narrow strip of region surrounding this cusp does not correspond to a bundle of classical trajectories unlike in the case of the Wannier ridge of the real hydrogen. Nonetheless, the local semiquantal treatment of the ridge still applies and is conducive to the remarkable exponential law. Our work has provided pieces of evidence that support this picture.

A nontrivial connection between the Coulomb and asymptotic zones appears observable even in real systems. Indeed, it is difficult to make a compromise between the uniform energy distribution in $e+H\rightarrow e+e+p$ and the uniform spatial distribution of the electron pair in the Coulomb zone. A classical theory of Peterkop and Liepinsh [21] elucidated that the spatial distribution is approximately proportional to $\sin 2\alpha$, i.e., far from uniform. In classical terms, the above observation suggests for the ''real'' ionization that the trajectories concentrated near the potential ridge tend to spread into the asymptotic zone in such a way that more trajectories tend to remain near the ridge. What is surprising

is that this tendency follows the $\sin 2\alpha$ behavior more closely than one would naively expect [22,3]. This as well as the remarkable V-shaped energy distribution of the Temkin-Poet [11,12] model may reflect a hitherto unexplained mechanism joining the Coulomb and asymptotic zones.

We wish to thank Professor M. Matsuzawa for his encouragement and interest throughout this work. We also thank Dr. I. Bray for providing his results prior to publication. This work was supported in part by a Grant-in-Aid, Ministry of Education, Science and Culture, Japan.

[1] I. Bray, Phys. Rev. Lett. **78**, 4721 (1997).
[2] D. Kato and S. Watanabe, Phys. Rev. Lett. **74**, 2443 (1995).
[3] D. Kato and S. Watanabe, J. Phys. B **29**, L779 (1996); Phys. Rev. A **56**, 3687 (1997). See also S. Watanabe, D. Kato, and M. Matsuzawa, Comments At. Mol. Phys. **33**, 95 (1996).
[4] G. Wannier, Phys. Rev. **90**, 817 (1953).
[5] A. R. P. Rau, Phys. Rev. A **4**, 207 (1971).
[6] R. Peterkop, J. Phys. B **4**, 513 (1971).
[7] U. Fano, Phys. Rev. A **22**, 2660 (1980).
[8] S. Watanabe, J. Phys. B **24**, L39 (1991).
[9] J. H. Macek and W. Ihra, Phys. Rev. A **55**, 2024 (1997).
[10] The allowed space makes it impossible to complete an author list. Only a few are mentioned as a suggestion for the reader. For instance, see J. M. Feagin, J. Phys. B **28**, 1495 (1995); D. S. Crothers, *ibid.* **19**, 463 (1986); F. H. Read, *ibid.* **17**, 3965 (1984).
[11] A. Temkin, Phys. Rev. **126**, 130 (1962).
[12] R. Poet, J. Phys. B **11**, 3081 (1978).
[13] G. Handke, M. Draeger, W. I. Ihra, and H. Friedrich, Phys. Rev. A **48**, 3699 (1993).
[14] Although there is a simple scaling argument that produces the appropriate R dependence of the optical potential, it appears more profitable instead to resort to the following general argument. The equation of motion for the adiabatic channel functions: $[\partial^2/\partial\alpha^2+2RC_0+2R\,\kappa(\pi/4-\alpha)^n]\Phi=-2U(R)\Phi$, where C_0 and κ are constants, and may be solved for Φ by the WKB approximation up to the point $\tilde{\alpha}$ where $2RC_0+2R\,\kappa(\pi/4-\tilde{\alpha})^n=-2U(R)$, which marks the *asymptotic* region with respect to α. The boundary condition that the solution be outgoing leads to a complex-valued potential that scales as $R^{-2(1+n)/(2+n)}$. Importantly, this argument based on the standard adiabatic channel equation above is not limited to the series expansion of the potential surface about the ridge.
[15] Unlike the real hydrogen atom, there is no need for the Bogoliubov [8] transformation to incorporate the nonadiabatic effects to this order.
[16] A. Temkin, Phys. Rev. Lett. **16**, 835 (1966); and (unpublished).
[17] F. Robicheax, M. S. Pindzola, and D. R. Plante, Phys. Rev. A **55**, 3573 (1997).
[18] M. P. Scott, P. G. Burke, K. Barschat, and I. Bray, J. Phys. B **30**, L309 (1997). Their fitted coefficient γ differs from ours by about factor of 2. This is most likely due to their matching radius set to 150 a.u., too small for resolving the threshold energy region for an unequivocal determination of γ.
[19] J. M. Rost, Phys. Rev. Lett. **72**, 1998 (1994).
[20] R. Peterkop, *Theory of Ionization of Atom by Electron Impact* (Colorado Associated University Press, Boulder, 1977).
[21] R. Peterkop and A. Liepinsh, J. Phys. B **14**, 4125 (1981).
[22] For instance, A. K. Kazansky, V. N. Ostrovsky, and L. Yu. Sergeeva, J. Phys. B **19**, 5197 (1994); J. H. Macek (private communication).